INVESTIGATOR'S BROCHURE

3'-deoxy-3'-[F-18] fluorothymidine: [F-18]FLT

An Investigational Positron Emission Tomography (PET) Radiopharmaceutical for Injection intended for use as an in vivo diagnostic for imaging active cellular proliferation of malignant tumors.

Investigational New Drug (IND) Application
IND # 71,260

Put your institution name and address here

Edition Number: 7
Edition Date: August 2009

I. TABLE OF CONTENTS ... 2

II. INTRODUCTION ... 3

III. [F-18]FLT PRODUCT AGENT DESCRIPTION ... 3

1. Agent Description ... 3
2. Chemical Structure ... 4
3. Final Product Specifications ... 5

IV. PHARMACOLOGY ... 6

V. TOXICOLOGY AND SAFETY ... 6

1. Mechanism of Action for Toxicity ... 6
2. [F-19] FLT Animal Toxicity Studies ... 6
3. [F-18] FLT Animal Toxicity Studies ... 8
4. [F-19] FLT Human Toxicity ... 8
5. [F-18] FLT Human Toxicity Studies ... 9
6. [F-18] FLT Human Safety Studies ... 9
7. [F-19] Genotoxicity and Mutagenicity ... 13
8. Adverse Events and Monitoring for Toxicity ... 13
9. Safety and Toxicity of the Other Components of the Final [F-18] FLT Drug Product ... 14

VI. BIODISTRIBUTION AND RADIATION DOSIMETRY OF [F-18] FLT ... 15

1. Mouse Biodistribution ... 15
2. Non-Human Primate Biodistribution ... 15
3. Human Radiation Dosimetry of [F-18]-FLT ... 16

VII. [F-18]FLT PREVIOUS HUMAN EXPERIENCE ... 22

VIII. REFERENCES ... 27

II. INTRODUCTION

3'-deoxy-3'-[F-18] fluorothymidine [F-18]FLT is a structural analog of the DNA constituent, thymidine, that enters proliferating cells and is phosphorylated by human thymidine kinase 1, which is regulated during the cell cycle. The 3' substitution prevents further incorporation into replicating DNA, and the now ionic [F-18]FLT-MP is trapped inside proliferating cells. [F-18] decays with positron emission.

Positron Emission Tomography

Positron emission tomography (PET) is a quantitative tomographic imaging technique which produces cross-sectional images that are composites of volume elements (voxels). In PET images, the signal intensity in each voxel is dependent upon the concentration of the radionuclide within the target tissue (e.g., organ, tumor) volume. To obtain PET imaging data, the patient is placed in a circumferential detector array.

Patients will undergo 2 separate components for a typical PET imaging procedure. One component is a transmission scan via a germanium rod source or, more recently, by CT imaging (in the case of PET-CT) over the field-of-view of interest (specifically the tumor or the majority of the body with whole body PET/PET-CT imaging). The second component of the study is the emission scan which can be a dynamic imaging acquisition over a specific area of interest or multiple acquisitions over the whole body. The typical PET study takes about 20 minutes to 2 hours to perform depending on the nature of the acquisitions and the areas of the body that are imaged.

The patient is often prepared by fasting for 4-6 hours. After the [F-18] FLT tracer (approximately 5 mCi) is injected, imaging can commence immediately for a fully quantitative study over one area of the body, or imaging can be performed after an uptake period of about 60-90 minutes if whole body semi-quantitative imaging is being performed.

Although [F-18]FLT studies are designed to characterize FLT as a tracer of cellular proliferation in the primary tumor, comparison of [F-18]FLT images with other clinical imaging, and with surgical staging, will also provide data about [F-18]FLT's ability to depict regional tumor proliferation and distal metastases.

III. [F-18]FLT PRODUCT AGENT DESCRIPTION

1. AGENT DESCRIPTION

3'-deoxy-3'-[F-18]fluorothymidine: [F-18]FLT (MW 243) is a structural analog of the DNA constituent, thymidine (Figure 1). It is a radiolabeled imaging agent that has been proposed for investigating cellular proliferation with positron emission tomography (PET). Since FLT is not incorporated into DNA, due to phosphorylation by thymidine kinase, (a part of the proliferation pathway) FLT-monophosphate (FLT-MP) is trapped in

the cell. As such, it has the potential to facilitate imaging of proliferating tumor in proportion to the DNA synthesis rate. Clinical and nonclinical studies support the use of FLT as an imaging probe for quantifying cellular proliferation with positron emission tomography (PET). Therefore, FLT is proposed as a radiolabeled imaging probe for quantifying cellular proliferation in malignant tumors with PET.

2. CHEMICAL STRUCTURE

[F-18]FLT has not been marketed in the United States and, to the best of our knowledge; there has been no marketing experience with this drug in other countries. The radiopharmaceutical product, [F-18]FLT is the only active ingredient and it is dissolved in a solution of ≤ 10 mL of 92% 0.01 M phosphate buffered saline (PBS): 8% ethanol (v:v). The drug solution is stored at room temperature in a gray butyl septum sealed, sterile, pyrogen-free glass vial with an expiration time of 8 hours. The injectable dose of [F-18]FLT for most studies will be approximately 175 MBq (5 mCi) at the time of injection. In the dose of [F-18]FLT only a small fraction of the FLT molecules are radioactive. The amount of injected drug is ≤ 0.61 μg/mL (≤ 2.5 nmol/mL) of FLT. [F-18]FLT is administered to subjects by intravenous injection of ≤ 10 mL.

There is no evidence that nonradioactive and radioactive FLT molecules display different biochemical behavior.

Figure 1

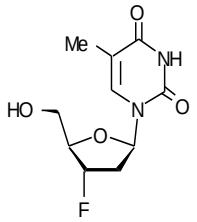

FLT

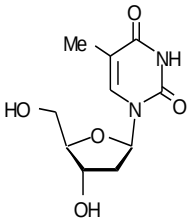

Thymidine

3. FINAL PRODUCT SPECIFICATIONS

The drug is composed of a small amount of [F-18]FLT that is labeled with radioactive F-18 at the 3'-position on the sugar ring with a specific activity ranging < 200 Ci/mmol at the time of injection. The radiopharmaceutical product, [F-18]FLT is the only active ingredient and it is dissolved in a solution of ≤ 10 mL of 92% 0.01 M phosphate buffered saline (PBS): 8% ethanol (v:v). [F-18]FLT is administered to subjects by intravenous injection (≤ 10 mL).

Table 1. Final Product Specifications

Radiochemical Purity(TLC):	R_f = 0.4-0.7 Purity ≥ 95%
Residual Solvent Levels:	Acetone < 5000 ppm Acetonitrile < 400 ppm DMSO < 5000 ppm
Radionuclidic Purity:	Measured half-life 100-120 minutes
Bacterial Endotoxin Levels:	< 175 EU per dose
pH:	6-8
Sterility:	no growth observed in 14 days
Residual Kryptofix® [2.2.2]:	< 50 µg/ mL Kryptofix®
Radiochemical Purity (HPLC)	> 95%
Chemical Purity (HPLC):	FLT < 0.61 µg /ml Other < 1.2 µg/ml
Chemical Purity (particulates):	Clear and Colorless

Table 2. Final Product Components

COMPONENTS		
[^{18}F]FLT, 3'-deoxy-3'-[^{18}F]fluorothymidine	same as for [F-19]FLT	≤ 5.0 mCi
[^{19}F]FLT, 3'-deoxy-3'-[^{19}F]fluorothymidine	NSC #140025 for [F-19]FLT	≤ 0.61 µg/ml
Sodium phosphates	USP	0.01 M (92% by volume)
Ethanol, absolute	USP	8% by volume
Saline for injection	USP	0.15 M

Table 3. Final Product Impurities

IMPURITIES		**Highest values in two site Qualification Runs (n=17)**
Kryptofix [2.2.2.]	< 50 µg/ml	None detected
Acetonitrile	< 400 ppm	86 ppm
DMSO	< 5000 ppm	353 ppm
Acetone	< 5000 ppm	190 ppm

IV. PHARMACOLOGY

The pharmacology of FLT is based on its action as an inhibitor of DNA synthesis (Langen, 1969; 1972; 1972; Matthes, 1988). Intracellular metabolism of FLT produces nucleotides that inhibit endogenous DNA polymerases because they lack a 3'-hydroxyl substituent. This results in premature chain termination of DNA synthesis (Matthes 1987, Sundseth 1996). These biochemical properties can account for FLT's prominent hematological and liver toxicity in treatment studies. The proposed PET tracer studies using approximately 6 μg single dose [F-18]FLT are significantly lower than the oral 0.125 mg/kg or 2 mg/day multi dose used in the human studies (Flexner, 1994; Faraj, 1994; Sundseth, 1996; Katlama, 2004; Ghosn, 2007). The pharmacology of FLT closely parallels that of the widely used prescription HIV-antiviral drug azidothymidine (AZT) (Lundgren, 1991; Kong, 1992). Both FLT and AZT are 3'-deoxythymidine analogs that act as inhibitors of DNA synthesis and are cleared from the body in the same way. Although FLT is significantly more cytotoxic than AZT in test cell lines (Faraj, 1994) at comparable levels of exposure, this is not a factor when [F-18]FLT exposure is limited to typical PET imaging microdose requirements. Cellular uptake of FLT and thymidine is greater than that of AZT. Transport of FLT and thymidine across cell membranes occurs by active transport and passive diffusion (Kong, 1992).

V. TOXICOLOGY AND SAFETY

1. MECHANISM OF ACTION FOR TOXICITY

Intracellular metabolism of FLT produces nucleotide phosphates that inhibit endogenous DNA polymerases and can prematurely chain terminate DNA (Matthes, 1987; Sundseth, 1996). These biochemical properties can account for FLT's prominent hematological and liver toxicity when dose at high dose in treatment studies. The proposed PET tracer studies using approximately 6 μg single dose [F-18]FLT are a thousand fold lower than the oral 0.125 mg/kg multi dose used in the human studies (Flexner, 1994; Faraj, 1994; Sundseth, 1996; Katlama, 2004; Ghosn, 2007).

2. [F-19] FLT ANIMAL TOXICITY STUDIES

A preliminary study of FLT's toxic effects was reported for Cynomologus monkeys receiving multiple doses of FLT by subcutaneous injection (3 x 0.25 mg/Kg s.c.; Lundgren, 1991). Table 4 lists the wide variety of standard hematological parameters, liver enzymes, and serum creatinine for the FLT treated monkeys and controls that were studied.

Table 4. Laboratory Values for Cynomologus Monkey Study

	DAY 1	DAY 0	DAY 10		DAY 41	
Analyte	FLT	CONTROL	FLT	CONTROL	FLT	CONTROL
Albumin (g/L)	32	32	32	32	40	32
Creatinine (µmol/L)	83	88	68	75	76	75
GGT (µkat/L)	1.03	1.60	0.62	1.26	0.82	1.58
SGOT (µkat/L)	0.60	1.53	0.95	1.36	0.68	0.72
SGPT (µkat/L)	2.11	2.67	1.61	2.11	1.05	1.45
CK (µkat/L)	6.78	4.17	5.70	2.64	8.02	5.53
LDH (µkat/L)	33	36	29.2	35.2	28.5	25.2
WBC ($x10^{-9}$/L)	4.92	8.2	4.72	7.5	5.84	9.52
RBC ($x10^{-12}$/L)	6.06	5.6	4.9	4.71	5.74	5.78
HGB (g/L)	112	102	89	85	105	103
HCT	0.37	0.35	0.30	0.29	0.36	0.36
PLT ($x10^{-9}$/L)	332	414	246	348	352	430
MCV (fl)	61.6	62.9	59.8	62.0	62.0	62.1

Standard hematological parameters, liver enzymes and serum creatinine values for FLT treated (3 x 0.25 mg/Kg; s.c.: n=2) and controls (n=4) for Cynomologus monkeys. (1.0 kat/l = 58.8U/L)

Unpublished studies filed to the NCI IND (studies are the property of Medivir) in mice, rats and dog reported only minor hematological effects at doses up to 900 mg/kg iv in mice and rats and 1000 mg/kg iv in dogs.

3. [F-18] FLT ANIMAL TOXICITY STUDIES

There are currently no published animal toxicity data for [F-18] FLT. Since the half life of Fluorine18 is only 109 minutes toxicity studies are not possible with the radiolabeled agent. The [F-19] data presented would be the basis for both animal and human toxicity characterization.

4. [F-19] FLT HUMAN TOXICITY

The pharmacology of FLT is based on its action as an inhibitor of DNA synthesis (Langen, 1969; 1972; 1972; Matthes, 1988). This is the mechanism of the toxicity that is seen with the drug. Intracellular metabolism of FLT produces FLT-phosphates but these nucleotides inhibit endogenous DNA polymerases because they lack a 3'-hydroxyl substituent. This results in premature chain termination of DNA synthesis (Matthes 1987, Sundseth 1996). These biochemical properties can account for FLT's prominent hematological and liver toxicity (Flexner, 1994; Faraj, 1994; Sundseth, 1996). The pharmacology of FLT closely parallels that of the widely used prescription HIV-antiviral drug azidothymidine (AZT) (Lundgren, 1991; Kong, 1992). Both FLT and AZT are 3'-deoxythymidine analogs that act as inhibitors of DNA synthesis and are cleared from the body in the same way. However, FLT is significantly more cytotoxic than AZT in test cell lines (Faraj, 1994). Cellular uptake of FLT and thymidine is greater than that of AZT. Transport of FLT and thymidine across cell membranes occurs by active transport and passive diffusion (Kong, 1992).

FLT was investigated as an oral anti-AIDS drug in humans (Flexner 1994). Toxic effects and death were reported for some subjects receiving FLT during randomized concentration controlled trials during a 16-week treatment of oral multi-dosing. Doses of 0.125 mg/kg every 12h, produced a mean cumulated drug exposure (AUC_{12}: area under curve) of 417 ng-h/mL. At this level, serious (grade 3) hematologic toxicity occurred in 6 of 10 subjects. At 300 ng-h/mL, grade 2 or greater (fall in hemoglobin to ≤ 9.4 g/dL) anemia developed within 4 weeks in 9 of 12 subjects. At 200 ng-h/mL almost no clinically significant anemia developed, but dose-limiting granulocytopenia (< 750 granulocytes/mm^3) occurred in 5 of 14 subjects. Mild peripheral neuropathy occurred in 2 of 15 subjects at 50 ng-h/mL, but was not dose-limiting.

FLT drug trials were terminated after 2 subjects died unexpectedly of hepatic failure. One of these subjects, who was assigned to 200 ng-h/mL, developed progressive liver failure and died after 12 weeks of FLT therapy. A second subject, receiving a fixed dose of 10 mg/day, developed progressive liver failure and died at 12 weeks. All surviving subjects were followed closely for 4 weeks after stopping FLT and none had evidence of clinically significant liver disease or other adverse effects. Overall, 25 of the 44 subjects receiving at least two doses of FLT, completed the 16 week study without clinically significant adverse effects.

FLT (Alovudine) was withdrawn from development for several years, and then reinvestigated for multi-drug resistant HIV infection. Fifteen patients with multi-drug resistance HIV received 7.5 mg each day for 28 days along with their on-going therapy (Katlama, 2004). No serious adverse events were observed.

A randomized, double-blind, placebo-controlled trial investigating three doses of alovudine (0.5, 1 and 2 mg) or placebo added for 4 weeks to a failing regimen in patients with evidence of NRTI resistant HIV strains. Seventy-two patients were enrolled in the study: 21, 13, 18 and 20 in the placebo and 0.5, 1 and 2 mg arms, respectively. There was no significant change in CD4 cell count. Alovudine was well tolerated; diarrhea and nausea were reported in up to one-third of the patients and mean hemoglobin decreased slightly in the highest dose group. (Ghosn, 2007)

5. [F-18] FLT HUMAN TOXICITY STUDIES

Since the half life of fluorine 18 is only 109 minutes toxicity studies are not possible with the radiolabeled agent. The [F-19] data presented would be the basis for both animal and human toxicity characterization.

It is important to note that [F-19] clinical repeat dosing, as reported above, results in total exposure that is up to several thousand times greater, as measured by AUC_{12}, than that produced by typical [F-18] dosing in a PET imaging setting.

6. [F-18] FLT HUMAN SAFETY STUDIES

In a recent study performed at the University of Washington, Turcotte and colleagues (Turcotte, 2007) assessed the toxicity of [F-18]FLT in twenty patients with proven or suspected diagnosis of non-small cell lung cancer (Table 5). All patients gave written informed consent to the [F-18]FLT injection, subsequent PET imaging and blood draws. Blood samples were collected for each patient at multiple times before and after [F-18]FLT-PET. These samples were assayed for comprehensive metabolic panel, total bilirubin, complete blood and platelet counts. In addition, a standard neurological examination by a qualified physician was performed for each patient before and immediately after [F-18]FLT-PET. All [F-18]FLT doses were calculated based on patient weight (2.59 MBq/kg = 0.07 mCi/kg) with a maximal dose of 185 MBq (5.0 mCi). Starting with the [F-18]FLT injection, dynamic PET images were acquired for 90 or 120 minutes. By placing a region-of-interest in the center of the left ventricular chamber, blood time-activity curves were generated for each patient from the dynamic PET data and then extrapolated to 720 minutes. This provided a measure of the area under the [F-18]FLT concentration curve for 12 hours (AUC_{12}). A separate estimation of the AUC_{12} was also obtained from sequential blood samples collected during PET data acquisition. No side effects were reported by patients or observed. No change was observed in the neurological status of patients. A neurological examination was performed by an experienced neurologist prior to [F-18]FLT administration, the day after [F-18]FLT administration, and at 4 weeks post [F-18]FLT administration. Only albumin, red blood cell count, hemoglobin, and hematocrit show a statistically significant decrease over

time (Table 5). These changes were attributed to IV hydration during PET imaging and to subsequent blood loss at surgery. The AUC_{12} values estimated from imaging data are not significantly different from those found from serial measures of [F-18]FLT blood concentrations (P= 0.66). No significant neurologic sequelae have been attributed to [F-18]FLT use in pet imaging to date. As a result, peripheral neuropathy, which had been listed as a possible risk based upon observations at significantly higher doses in early therapeutic HIV studies, is no longer considered a risk of [F-18]FLT use in a micro-dose imaging setting. Screening for peripheral neuropathy is not justified based upon the available evidence in multiple [F-18]FLT imaging trials.

Table 5. Laboratory values (mean ± SD) at each time point

	Pre-[F-18]FLT	Immediate <5h	5-24 Hours	1-7 days	> 1week	P*
Sodium (mEq/L ±SD)	139.4 ± 1.5	138.2 ± 2.1	138.3 ± 2.0	137.5 ± 1.8	138.1 ± 2.3	0.064
Potassium (mEq/L ±SD)	4.2 ± 0.5	4.2 ± 0.4	4.1 ± 0.4	4.2 ± 0.3	4.2 ± 0.4	0.968
Chloride (mEq/L ±SD)	102.3 ± 3.3	104.2 ± 3.7	104 ± 3.8	102.3 ± 2.4	101.2 ± 3.1	0.055
Glucose (mEq/L ±SD)	95.1 ± 14.8	96.6 ± 20.7	98.5 ± 23.1	105.4 ± 17.7	109.5 ± 14.6	0.175
Creatinine (mEq/L ±SD)	0.885 ± 0.198	0.882 ± 0.207	0.881 ± 0.180	0.910 ± 0.190	0.844 ± 0.217	0.949
BUN (mEq/L ±SD)	15.8 ± 5.0	15.1 ± 5.6	15.2 ± 6.3	14.3 ± 5.2	15.3 ± 5.7	0.959
SGOT (U/L ±SD)	20.8 ± 5.0	22.0 ± 5.1	22.0 ± 5.3	22.2 ± 11.4	21.8 ± 6.7	0.973
SGPT (U/L ±SD)	18.7 ± 6.7	18.5 ± 6.6	19.1 ± 6.5	17.6 ± 5.3	17.2 ± 6.5	0.978
Albumin (g/dL ±SD)	3.9 ± 0.5	3.5 ± 0.4	3.44 ± 0.3	3.1 ± 0.6	3.2 ± 0.8	0.003
Alk Phos (U/L ±SD)	73.8 ± 19.4	61.1 ± 14.7	58.3 ± 17.0	59.5 ± 22.7		0.081
Bilirubin (mg/dL ±SD)	0.647 ± 1.81	0.573 ± 0.246	0.581 ± 0.263	0.621 ± 0.286	0.752 ± 0.418	0.714
RBC ($X10^9$/ml ±SD)	4.5 ± 0.4	4.3 ± 0.5	4.2 ± 0.5	3.8 ± 0.3	3.7 ± 0.4	<0.0001
Hematocrit (% ±SD)	40.9 ± 3.1	39.1 ± 4.4	38.4 ± 4.0	35.2 ± 3.4	35.0 ± 3.4	<0.0001
WBC ($X10^6$/ml ±SD)	7.6 ± 2.1	7.7 ± 3.4	7.9 ± 3.3	9.5 ± 2.8	9.0 ± 3.2	0.262
Platelets ($X10^6$/ml ± SD)	278.1 ± 96.9	259.1 ± 103.1	255.9 ± 103.0	230.1 ± 76.7	233.5 ± 69.5	0.674

*one-way ANOVA P values (from Turcotte et al, 2007)

The single dose AUC12 values derived from blood clearance studies performed at the University of Washington ranged from 0.22 to 1.34 ng-h/mL with a mean of 0.80 ng-h/mL. This range corresponds to 0.46% to 2.7% of the Flexner therapeutic clinical trial AUC_{12} of 50 ng-h/mL. In the Flexner trial the only dose-limiting toxicity was hematologic, either anemia or granulocytopenia, and the threshold for this response was greater than 50 ng-h/mL. The only adverse event at the 50 ng-h/mL level was a peripheral neuropathy in 2 of 15 patients that manifested at about 40 days. The peripheral neuropathy was detected by vibration sensation scores and was not a dose limiting toxicity. For FLT, the average arterial blood curve (% injected dose per mL of blood) from 16 University of Washington FLT 2 hr studies were extrapolated to 12 hours using the conservative estimation that there would be no more clearance of FLT from the plasma and that all the radioactivity in the blood was in the form of the unmetabolized FLT. It was then assumed that 100% of the dose (6.1 µg = 6100 ng) was in a plasma volume of 3,000 mL. The dose in nanograms was multiplied by the fraction

of the injected dose per mL divided by the plasma volume to obtain ng/mL for each time point. The area under this curve was 0.5 ng-h/mL. Thus, the AUC_{12} of a single injected dose of FLT will be <1% of the single dose and less than 0.01% of the cumulative 40 day dose of the lowest mass associated with any reported toxic effect in humans, 50 ng-h/mL and will not lead to clinically detectable toxic effects.

An NCI-sponsored study (Spence, 2008) was conducted at University of Washington in Seattle beginning in 2005. Twelve patients with brain tumors were enrolled. Overall, 2 of the 12 subjects receiving FLT experienced an elevation in BP from baseline to 2 hours post infusion subjects 1 (119/56 – 133/66) and 4 (120/78 – 163/74). In Subject 4, abnormal BP was attributed to discomfort from the head immobilization device. There were no clinically relevant events reported. All subjects performed consistently on the pre and post neurological exams and there were no changes in status. The clinical chemistry data are shown in Table 6.

Four of these analytes demonstrated statistically significant changes on one-way ANOVA: potassium, carbon dioxide, total protein, and albumin. Some of the other values were above or below normal, but no pattern was seen except that many were lower on the day of the study. These decreases are attributed to two main factors. Normal saline infusion, which expands blood volume, and arterial blood sampling for kinetic analysis are performed during the procedure, both of which will cause a general lowering of the concentration of blood components. The subsequent recovery of these values to baseline is consistent with this explanation and consistent with the results obtained by Turcotte.

The AUC_{12} values, estimated from assaying arterial blood samples, ranged from 0.004 to 0.035 ng-hr/ml, with a mean of 0.016 ng-hr/ml. These mass levels correspond to 0.008% to 0.07% of the least toxic single dose of 50 ng-hr/ml in the Flexner trial (a 40 day, 2 dose per day study). If comparison is made to the cumulative dose, the [F-18]FLT is at 0.0001% to 0.0009% of the therapeutic dose.

Table 6. Laboratory values (mean ± SD) at each time point.

Analyte	Pre Mean ± SD	Immediately Pre-Mean ± SD	Day 1 Mean ± SD	Day 28 Mean ± SD
Amylase	75.4±23.1	68.5±27.6	77.8±33.9	75.4±33.7
Na+	140.8±2.6	138.4±4.6	139.3±3.3	141.1±3.1
K+	4.27±0.42	**3.88*±0.20**	4.20±0.28	4.08±0.30
Cl-	106.0±3.7	106.0±4.6	104.5±3.6	106.5±3.3
CO2 total	27.6±2.9	**24.6*±2.3**	26.9±2.1	26.8±2.5
Ion Gap	6.29±1.60	7.83±2.29	7.70±2.21	7.67±3.08
Glucose	121.8±47.7	98.7±33.4	125.2±73.5	116.9±71.6
BUN	12.45±4.06	10.58±4.01	11.00±3.03	13.73±4.63
Creatinine	1.00±0.17	0.85±0.17	0.97±0.24	1.01±0.27
Protein total	6.45±0.38	**5.66*±0.37**	6.14±0.57	6.33±0.76
Albumin	4.15±0.25	**3.66*±0.18**	4.01±0.51	3.99±0.50
Bilirubin total	0.68±0.16	0.79±0.24	0.79±0.17	0.65±0.12
Ca++	9.35±0.19	9.01±0.29	9.38±0.39	9.24±0.54
AST (GOT)	26.3±5.9	22.5±4.4	23.7±5.0	26.8±5.1
Alk Phos	86.0±22.7	78.5±26.4	84.3±27.9	86.5±30.3
GPT	39.4±15.8	30.2±9.6	32.7±11.2	33.0±7.7
GGT	44.7±21.1	42.3±22.4	47.2±23.3	44.3±26.0
LDH	224.9±104.9	151.8±41.9	174.9±57.9	248.6±205.4
Phosphate	3.15±0.55	3.03±0.55	3.16±0.59	3.07±0.41
Prothrombin	12.74±1.39	13.59±0.52	13.12±0.94	12.82±1.39
INR	1.02±0.04	1.05±0.05	1.01±0.09	1.01±0.06
PTT	26.8±3.1	29.4±5.7	30.9±15.8	26.3±2.8
WBC	6.13±1.91	5.75±1.40	6.96±3.98	5.85±2.10
RBC	4.65±0.42	4.37±0.39	4.50±0.38	4.48±0.52
Hgb	14.5±1.1	13.4±0.9	13.9±1.1	13.9±1.6
Hct	42.5±3.1	39.9±3.4	41.1±3.0	41.2±4.5
MCV	91.5±3.3	91.3±3.5	91.3±3.2	92.1±3.3
MCH	31.4±1.6	30.8±1.4	31.0±1.4	31.2±1.3
MCHC	34.3±0.9	33.7±0.8	33.9±0.6	33.9±0.8
Platelets	233.9±54.2	226.2±42.7	220.9±47.8	220.0±52.4
ANC	4.08±1.42	3.79±1.15	5.02±3.34	3.89±1.42
Spec Gravity	1.02±0.01	1.01±0.00	1.02±0.00	1.02±0.00
pH	6.05±1.01	6.88±0.80	6.60±0.97	5.85±1.08

* statistically significant change ($p<0.05$); one-way ANOVA

7. [F-19] GENOTOXICITY AND MUTAGENICITY

There are some literature reports on the mutagenic properties of FLT. Ehrlich ascites tumor cells incubated with 10 µM FLT for extended periods (12, 24, 36 h: AUC 120, 240, 360 nmol-h/mL) showed chromosome damage (Wobus 1976). The most prominent effects were breaks and gaps, however, much less damage was seen if a recovery time was included (12, 24 h) and the damage could also be largely reversed by post-treatment with thymidine (10 µM). FLT anabolism, FLT incorporation into DNA and the effects of FLT on cellular genome integrity have been studied in cultured CEM ($CD4^+$ human lymphoblastoid) cells (Sundseth 1996). FLT concentrations of 10 and 100 µM produced chromosome fragmentation characteristic of cells undergoing apoptosis. In contrast, at 1 µM FLT the level of fragmentation was similar to the controls without FLT exposure. Despite prominent levels of intracellular FLT anabolites, the fraction of FLT in DNA was low (10^{-6} total). At the lowest acceptable FLT specific activity (200 Ci/mmol), the dose to patients (5 mCi) will correspond to an initial, maximal plasma concentration of about 5 nM. This is 200 times lower than the level of FLT where no chromosomal damage was seen in CEM cells (1 µM). Based on these data, the administration of approximately 5 mCi of FLT to humans does not pose a probable threat of mutagenesis.

8. ADVERSE EVENTS AND MONITORING FOR TOXICITY

As discussed above, the mechanism of action of FLT's toxicity at therapeutic dosing levels is based on inhibition of DNA synthesis (Langen, 1969; 1972; 1972; Matthes; 1988). Total exposure to the radiolabeled agent for PET imaging, will be several thousand times lower than the exposure at which toxicity has been observed in humans. Nevertheless, as with all investigational drugs, patients receiving FLT should be observed for adverse events, and promptly treated should any adverse effects occur.

In the Flexner HIV therapeutic dosing study mild peripheral neuropathy occurred in 2 of 15 subjects at 50 ng-h/mL, but was not dose-limiting. In the Katlama study, no serious adverse events were observed. Four patients experienced fatigue, three experienced loss of appetite, two grade 1 and one grade 2 transaminase elevations and one fall in hemoglobin. In a recent randomized, double-blind placebo-controlled study of NRTI-resistant HIV patients a four week course of 2 mg/day FLT significantly reduced their viral load and showed no significant signs of toxicity (Ghosn, 2007.)

In considering potential adverse effects that may be reasonably anticipated, based upon the available evidence for [F-18]FLT use in imaging, it is critical to note that for a single imaging study, at the lowest acceptable [F-18] FLT specific activity (200 Ci/mmol), the dose to patients (≤ 5.0 mCi) will correspond to an FLT injected mass of 25 nmoles. This is 10,000 times less than the cumulative dose, and 100 times lower than the level of FLT used in the therapeutic patient studies.

Based on these data, the administration of a total 10-15 mCi of [F-18]FLT over several imaging time points required to assess the effects of therapeutic intervention (baseline and typically

two time points during therapy) to humans poses a minimal risk for an adverse effect. Therefore, the risk profile for [F-18] FLT used as described in this Investigators Brochure consists of allergic reaction/anaphylaxis, which appears to be highly unlikely, and risks that would be associated with any clinical IV infusion/injection.

9. SAFETY AND TOXICITY OF THE OTHER COMPONENTS OF THE FINAL [F-18] FLT DRUG PRODUCT

The [F-18] FLT is purified by HPLC using an eluent of 8% ethanol. The maximum dose is 10 mL of 8% ethanol, or a maximum of 0.8 mL of ethanol, less than 5% of the amount of ethanol in one beer. In RTECs the LDLo is given as 1.4 g/kg orally for producing sleep, headache, nausea and vomiting. Ethanol has also been given intravenously to women experiencing premature labor (8 g/kg) without producing any lasting side effects (Jung 1980). Based on these reports, ethanol will not pose any danger of toxicity in this study.

The other components of the final product solution are, sterile water for injection, saline and 0.01 M phosphates, all USP grade. These are all nontoxic at the concentrations in the final drug. The final product is at pH 7 and the final injection volume is ≤10 mL.

The potential contaminants in the final [F-18] FLT drug product are: acetone, acetonitrile, dimethylsulfoxide, benzoate, Kryptofix® [2.2.2], other reaction products and excess unlabeled FLT.

Residual solvents in the final product are limited to 5,000 ppm (µg/mL) of acetone, 400 ppm of acetonitrile, and 5,000 ppm of dimethylsulfoxide (DMSO). DMSO is the solvent for the FLT precursor. Acetone is used to clean the TRACERLab FX_{F-N} system. Acetonitrile is used to dissolve the Kryptofix® [2.2.2]. The permissible level of acetonitrile in the final product is less than or equal to 400 ppm. This value is the same as that for the USP permissible level of acetonitrile in 2-[^{18}F]FDG which may not exceed 400 ppm. The allowable levels for both acetone and DMSO are less than 5,000 ppm. Both of these are Class 3 solvents; this class of solvents includes no solvent known as a human health hazard at levels normally accepted in pharmaceuticals. This limit is based upon the FDA's Guidance for Industry ICH Q3C-Tables and List (November 2003 Revision 1), page 7, where it considers 5,000 ppm in 10 mL i.e., 50 mg or less per day, of these Class 3 residual solvents as an acceptable limit, without additional justification. All of the residual solvent levels met our acceptance criteria in our initial qualification syntheses (n=17) at two sites.

The toxicity for Kryptofix® [2.2.2] has not been reported (RTECS Number Kryptofix ® 222 MP4750000) although this reagent has been investigated as a therapeutic in mice for chelation therapy after strontium exposure. The FDA has proposed a maximum permissible level of 50 µg/mL of Kryptofix® [2.2.2] in 2-[^{18}F]FDG, therefore this maximum permissible level will also apply to the [^{18}F]FLT final product.

Benzoic acid or sodium benzoate is the protecting group on the FLT organic precursor and is a potential contaminant in the final solution. The maximum amount of benzoic acid (the leaving group) possible in the final reaction is less than 3.5 mg, a nontoxic amount. The toxicity of benzoic acid and sodium benzoate was recently summarized in a final report (anonymous 2001). Sodium benzoate is a component of an approved intravenous solution (AMMONUL) given to newborn infants with hyperammonemia at a loading dose of 250 mg/kg.

The [^{18}F]FLT organic precursor does not elute from the analytical HPLC C18 column unless it is eluted with 35% methanol as opposed to the 14% methanol for the [^{18}F]FLT. It will behave the same on the preparative column. After synthesis the preparative HPLC column is washed with 70% ethanol to remove any retained organic material. Also, the FLT precursor should not survive the synthesis. Tests of the stability have confirmed the chemical degradation of the precursor during synthesis. For these reasons, the FLT organic precursor will not be in the final product.

Although the [^{18}F]FLT product is relatively pure, it is possible that trace amounts other reaction products might be found in the final product. The most likely is thymidine but other impurities are possible. For that reason an upper limit of 1.2 µg/ml has been set for any other materials in the final product that are retained more than 3 minutes on C18 HPLC and have UV absorbance at 254 or 266 nm. The 1.2 µg is determined by assuming that the UV absorbing compounds have the same molar extinction coefficient as FLT. Since FLT has a very high molar extinction coefficient (9,000 L mole^{-1}cm^{-1}) this is a conservative assumption.

VI. BIODISTRIBUTION AND RADIATION DOSIMETRY OF [F-18] FLT

1. MOUSE BIODISTRIBUTION

Preclinical development of [F-18]FLT was undertaken at the University of Washington; studying the uptake of FLT in cultured tumor cells, biodistribution studies with rodents (Rasey 2002) and monkeys and PET imaging in monkeys. Tumor cell cultures with a high S-phase fraction strongly sequester and retain labeled FLT and this uptake is proportional to the percentage of cells in S-phase. On this basis, imaging tumors with [F-18]FLT and modeling of data is designed to visualize regions of proliferation (high S-phase fraction).

2. NON-HUMAN PRIMATE BIODISTRIBUTION

Investigators at the University of Washington imaged four juvenile male monkeys (Macaca nemestrina): two normal monkeys and two acutely infected with human HIV. Approximately 4 mCi of [F-18]FLT was injected intravenously over 60 seconds and images were taken for 120 minutes. Blood samples were withdrawn via an arterial line, initially at 10 sec intervals and then at progressively longer times. This study provided estimates of organ specific dosimetry in a species closely related to man.

Table 7 shows the biodistribution data. They showed the following primary observations: (i) [F-18]FLT was avidly taken up in normally proliferating tissue, such as bone marrow; (ii) blood [F-18]FLT levels fell to low background levels within 20 min, (iii) [F-18]FLT and its primary metabolite cleared by the kidneys into urine (30-50% of the injected dose within 2 hours); (iv) the two HIV infected animals that were autopsied after imaging showed elevated levels of radioactivity (twice marrow levels) in lymphoid tissues, such as spleen and lymph nodes. These data are consistent with the more complete human data shown in the next section.

Table 7. [F-18]FLT biodistribution in juvenile male Macaca nemestrina infected with human HIV

SAMPLE/TISSUE	UPTAKE : Ci/g
Urine	18.00
Spleen	4.22* ; 3.86*
Ileum	2.04
Bone marrow	2.01 ; 1.78
Colon	1.67 ; 1.66
Jejunum	1.49
Duodenum	1.41
Liver	0.81 ; 0.65
Testes	0.27 ; 0.27
Muscle (right, left leg)	0.15 ; 0.13
Pectoralis	0.14 ; 0.13
Cerebellum	0.09
Brainstem	0.09
Cortex	0.08 ; 0.08

3. HUMAN RADIATION DOSIMETRY OF [F-18]-FLT

Eighteen patients (11 men, 7 women) with known or suspected lung cancer were prospectively studied with [F-18]FLT PET imaging at the University of Washington from March 2000 to April 2002 (Vesselle 2003). Biodistribution data from these 18 patient studies were used for dosimetry calculations. The age range was 45– 81 y (mean, 66 y) for men and 46 –75 y (mean, 62 y) for women. The weight range was 54 –126 kg (mean, 83 kg) for men and 46 –113 kg (mean, 75 kg) for women. The normal tissues in the imaging data that were used for dosimetry were distant from the site of any known tumor. During the course of the study, patients were hydrated with 500 mL of intravenous isotonic saline. All patients had normal renal function by medical history and as demonstrated by normal creatinine and normal blood urea nitrogen levels before PET. Two separate dynamic imaging sequences were used, either single or 2-field of view (FOV)

sequences. The imaging sequence for a single FOV protocol was eight 15-s, four 30-s, six 1-min, two 5-min, and ten 10-min imaging intervals. The imaging sequence for a 2-FOV (FOV1 and FOV2) protocol was four 25-s, three 50-s, three 2-min, and ten 5-min imaging intervals for FOV1 and four 25-s, three 50-s, three 2-min, and nine 5-min imaging intervals for FOV2. FOV1 imaging and FOV2 imaging were interleaved from the start of imaging with 15-s intervals taken to move between the 2 FOV's. This provided kinetic tracer uptake curves in the thorax region containing the primary tumor (FOV1) and within another region (FOV2) for dosimetry studies. The additional FOV was the pelvis in 6 patients (bladder, ovary, and testicular dosimetric information), the testes without the bladder in 1, the brain in 1, and the entire abdomen in 2 patients. Upper abdominal imaging was included within the thoracic FOV1 for patients with a thoracic lung lesion located in the lower lungs. Urine was collected at the end of each study.

ROIs were manually drawn within the boundaries of normal organs. The distribution of absorbed dose was calculated according to the MIRD method using the S values provided by the MIRDOSE3 software (ORISE; Oak Ridge, TN). The MIRD method assumes that the integrated activity is known for each of the source organs. Observed source organs where [F-18]FLT was concentrated were the urinary bladder, liver, kidneys, and bone marrow.

The integrated activity concentrations ($\tilde{C}$, MBq-h/g) were calculated for all organ ROIs using trapezoidal integration over time applied to the corrected time–activity curves over the duration of the dynamic dataset. A curve-fitting method was used to account properly for any outlying bladder time–activity curve and to allow calculation of urine reaccumulation after voiding. To test the effect of voiding on bladder dosimetry, two voiding scenarios were evaluated and applied to both male and female subjects.

The data for the residence times in organs using each of the voiding scenarios is noted below in Table 8 (men) and Table 9 (women). The first scenario is conservative, whereas the second has a more realistic voiding scheme. Scenario 1: Single bladder voiding at 6 h after [F-18]FLT administration with a 10% post-voiding bladder residual decayed to infinity. This scenario assumed no urine reaccumulation after 6 h. Scenario 2: First bladder voiding at 2 h after [F-18]FLT administration with a 10% post-voiding residual; urine reaccumulation between 2 and 6 h at a rate determined by the bladder curve fit; second bladder voiding at 6 h with a 10% post-voiding residual decayed to infinity. This scenario assumed no urine reaccumulation after 6 h.

Table **8. Cumulated Activity and Residence Time of [F-18]FLT for 5 mCi (185 MBq) Injection in a 70 kg Man.**

Source organ	*n*	$\tilde{C}$ (kBq-h/g)	SD $\tilde{C}$ (kBq-h/g)	Organ wt (g)	$\tilde{A} = \tilde{C}$ *x* wt (MBq-h)	SD $\tilde{A}$ (MBq-h)	tau (h)	SD tau (h)
Adrenals	1	1.93	0.339*	16.3	0.031	0.006	0.001	0.0002
Brain	1	0.229	0.040*	1420.0	0.325	0.057	0.009	0.0015
LLI	4	1.06	1.05	143.0	0.152	0.151	0.004	0.0041
Stomach	3	2.18	0.654	260.0	0.566	0.170	0.015	0.0046
Blood	11	1.14	0.198	454.0	0.516	0.090	0.014	0.0024
Heart wall	10	1.20	0.348	316.0	0.378	0.110	0.010	0.0030
Kidney	3	5.19	1.82	299.0	1.55	0.544	0.042	0.0147
Liver	6	6.17	1.64	1910.0	11.78	3.13	0.318	0.0847
Lung	11	0.572	0.157	1000.0	0.572	0.157	0.015	0.0042
Pancreas	2	2.37	1.59	94.3	0.223	0.150	0.006	0.0040
Marrow	11	7.70	2.27	1120.0	8.62	2.54	0.233	0.0688
Spleen	5	1.77	0.839	183.0	0.324	0.153	0.009	0.0041
Bladder† Void scenario 1	5	61.6	45.7‡	211.0	13.0	9.64	0.351	0.261
Void scenario 2		25.6			5.4		0.146	
Testes	3	1.36	0.753	39.1	0.053	0.029	0.001	0.001
Remainder§		0.872	0.160	66234.3	57.76	10.473	1.561	0.2831

* SD for organs with only 1 curve were calculated in proportion to SD of remainder.
† Bladder average and SD of 5 patients.
‡ SD for bladder was calculated from 5 patients with bladder curves.
§ Remainder of body for 73.7-kg man. Both voiding scenarios yield same remainder values.
wt weight; LLI lower large intestine.

Table **9. Cumulated Activity and Residence Time of [F-18]FLT for 4 mCi (147-MBq) Injection in a 56.8 kg Woman**

Source organ	n	$\tilde{C}$ (kBq-h/g)	SD $\tilde{C}$ (kBq-h/g)	Organ wt (g)	$\tilde{A} = \tilde{C}$ x wt (MBq-h)	SD $\tilde{A}$ (MBq-h)	tau (h)	SD tau (h)
Brain	1	0.406	0.064*	1410	0.572	0.090	0.015	0.0024
Breast	5	0.495	0.128	361	0.179	0.046	0.005	0.0012
LLI	1	0.913	0.150*	109	0.100	0.016	0.003	0.0004
Stomach	1	2.17	0.347*	195	0.423	0.068	0.011	0.0018
Blood	6	1.60	0.381	347	0.555	0.132	0.015	0.0036
Heart wall	6	1.71	0.341	241	0.413	0.082	0.011	0.0022
Kidney	1	6.07	1.55	248	1.50	0.389	0.041	0.0105
Liver	3	9.16	1.32	1400	12.83	1.85	0.347	0.0499
Lung	6	0.705	0.613	651	0.459	0.399	0.012	0.0108
Marrow	6	10.7	3.55	1050	11.24	3.73	0.304	0.101
Spleen	3	3.86	0.633	123	0.475	0.078	0.013	0.0021
Bladder‡ Void scenario 1	5	61.6	45.7	160	9.86	7.31	0.266	0.1976
Void scenario 2		25.6			4.09		0.111	
Remainder~		1.14	0.170	5050	57.7	8.43	1.56	0.228

* SD for organs with only 1 curve were calculated in proportion to SD of remainder.
† SD for kidney was calculated by pooling male and female kidney curves.
‡ Bladder average and SD of 5 patients.
§ SD for bladder was calculated from 5 patients with bladder curves.
~Remainder of body for 56.8-kg woman. Both voiding scenarios yield same remainder values.
wt weight; LLI lower large intestine.

The effective dose equivalent (EDE) for uniform whole-body exposure was calculated for both male and female weights, assuming a relative biologic effectiveness of 1.0 and following the procedure described in Addendum 1 to ICRP Publication 53. The dose estimates for the gonads, breast, red bone marrow, lungs, thyroid, bone surfaces, and remainder of body were multiplied by their weighting factors (0.25, 0.15, 0.12, 0.12, 0.03, 0.03, and 0.30, respectively) and summed to calculate the EDE. The weighting factor for the total body remainder was divided equally among the 5 remaining organs and tissues receiving the highest dose equivalent (weight of 0.06 per organ). For men, these were the urinary bladder wall, liver, kidneys, pancreas, and adrenal glands; for women, these were the urinary bladder wall, liver, kidneys, spleen, and uterus.

The organ dose estimates are presented in the Tables 10 (men) and 11 (women) including information based on the different voiding scenarios.

Table 10. Mean Organ Dose Estimates for Standard Man based on the two different voiding scenarios.

Organ	Scenario 1 (mean mGy/MBq)		Scenario 2 mean mGy/MBq)		SD (mGy/MBq)	
Adrenal	2.01E-02	(75)	2.07E-02	(77)	2.03E-03	(8)
Brain	3.25E-03	(12)	3.39E-03	(13)	3.72E-04	(1)
Breasts	8.13E-03	(30)	8.39E-03	(31)	9.24E-04	(3)
Gallbladder wall	1.65E-02	(61)	1.69E-02	(63)	2.12E-03	(8)
Lower large	1.51E-02	(56)	1.29E-02	(48)	4.55E-03	(17)
Small intestine	1.47E-02	(54)	1.42E-02	(53)	1.94E-03	(7)
Stomach	1.37E-02	(51)	1.41E-02	(52)	1.99E-03	(7)
Upper large	1.26E-02	(47)	1.24E-02	(46)	3.00E-03	(11)
Heart wall	1.62E-02	(60)	1.67E-02	(62)	2.00E-03	(7)
Kidney	3.52E-02	(13	3.56E-02	(132)	9.32E-03	(34)
Liver	4.51E-02	(16	4.54E-02	(168)	1.07E-02	(40)
Lungs	9.61E-03	(36)	1.01E-02	(37)	1.13E-03	(4)
Muscle	1.58E-02	(59)	1.68E-02	(62)	2.45E-03	(9)
Pancreas	2.24E-02	(83)	2.30E-02	(85)	7.63E-03	(28)
Red marrow	2.39E-02	(89)	2.40E-02	(89)	5.27E-03	(19)
Bone surface	1.55E-02	(57)	1.58E-02	(58)	3.04E-03	(11)
Skin	4.31E-03	(16)	4.44E-03	(16)	6.26E-04	(2)
Spleen	1.66E-02	(62)	1.71E-02	(63)	4.45E-03	(16)
Testes	1.45E-02	(54)	1.32E-02	(49)	4.34E-03	(16)
Thymus	1.05E-02	(39)	1.11E-02	(41)	1.11E-03	(4)
Thyroid	9.71E-03	(36)	1.04E-02	(38)	1.14E-03	(4)
Urinary bladder	1.79E-01	(66	7.91E-02	(293)	1.28E-01	(472)
Lens	9.97E-03	(36)	1.05E-02	(39)	1.15E-03	(4)
Total body	1.23E-02	(46)	1.26E-02	(47)	1.68E-03	(6)

Values in parentheses are mrad/mCi.
Scenario 1: bladder voiding at 6 h only (10% post-voiding residual decayed to infinity).
Scenario 2: bladder voiding at 2 and 6 h (10% residual after each voiding with re-accumulation of urine between 2 and 6 h. Residual urine decayed to infinity after 6 h).

Table 11. Mean Organ Doses for Women based on the two different voiding scenarios.

Organ	Scenario 1 (mean mGy/MBq)		Scenario 2 (mean mGy/MBq)		SD (mGy/MBq)	
Adrenal	2.01E-2	(74)	2.06E-02	(76)	1.58E-03	(6)
Brain	5.07E-03	(19)	5.21E-03	(19)	5.71E-04	(2)
Breasts	7.23E-03	(27)	7.47E-03	(28)	8.00E-04	(3)
Gallbladder wall	1.96E-02	(73)	1.99E-02	(74)	1.59E-03	(6)
Lower large	1.62E-02	(60)	1.40E-02	(52)	3.78E-03	(14
Small intestine	1.86E-02	(69)	1.80E-02	(67)	2.08E-03	(8)
Stomach	1.49E-02	(55)	1.53E-02	(57)	1.25E-03	(5)
Upper large	1.40E-02	(52)	1.36E-02	(50)	1.51E-03	(6)
Heart wall	2.23E-02	(83)	2.28E-02	(84)	2.17E-03	(8)
Kidney	4.20E-02	(155)	4.23E-02	(15	7.88E-03	(29
Liver	6.42E-02	(238)	6.45E-02	(23	8.38E-03	(31
Lungs	1.26E-02	(47)	1.31E-02	(49)	2.96E-03	(11
Muscle	2.37E-02	(88)	2.51E-02	(93)	3.01E-03	(11
Ovaries	2.07E-02	(77)	1.88E-02	(69)	3.65E-03	(14
Pancreas	1.96E-02	(72)	2.01E-02	(75)	1.44E-03	(5)
Red marrow	3.30E-02	(122)	3.31E-02	(12	8.47E-03	(31
Bone surface	2.00E-02	(74)	2.02E-02	(75)	4.43E-03	(16
Skin	5.07E-03	(19)	5.18E-03	(19)	5.95E-04	(2)
Spleen	2.89E-02	(107)	2.94E-02	(10	3.32E-03	(12
Thymus	1.35E-02	(50)	1.41E-02	(52)	1.17E-03	(4)
Thyroid	1.27E-02	(47)	1.33E-02	(49)	1.21E-03	(4)
Urinary bladder wall	1.74E-01	(646)	7.76E-02	(28	1.24E-01	(45
Uterus	2.53E-02	(94)	2.04E-02	(76)	7.20E-03	(27
Lens	9.18E-03	(34)	9.68E-03	(36)	8.77E-04	(3)
Total body	1.56E-02	(58)	1.59E-02	(59)	1.72E-03	(6)

The individual organ and total body doses associated with [F-18]FLT-PET are comparable to those for other comparable nuclear medicine procedures. The EDE for a 5 mCi dose in standard man is estimated to be 510 mrem (5.1 mSv) and for a standard female is 720 mrem (7.2 mSv).

A summary Table 12 of the relevant dosimetry is provided with the Total Body Exposure as well as the two other target organs of most concern. The bladder wall (independent on the voiding scenario) is the target organ with the liver receiving then next most significant radiation exposure in both man and woman.

Table 12. Summary of Dosimetry

Organ of Interest	Men mGy/MBq (mrad/mCi)	Woman mGy/MBq (mrad/mCi)
Total Body Dose	Scenario 1 1.23E-02 (46) Scenario 2 1.26 E-02 (47)	Scenario 1 1.56E-02 (58) Scenario 2 1.59 E-02 (59)
Bladder	Scenario 1 1.79E-01 (662) Scenario 2 7.91E-02 (293)	Scenario 1 1.74E-01 (646) Scenario 2 7.76E-02 (287)
Liver	Scenario 1 4.51E-02 (167) Scenario 2 4.54 E-02 (168)	Scenario 1 6.42E-02 (238) Scenario 2 6.45 E-02 (239)

Scenario 1: Single bladder voiding at 6 h after [F-18]FLT administration with a 10% post-voiding bladder residual decayed to infinity. This scenario assumed no urine reaccumulation after 6 h. Scenario 2: First bladder voiding at 2 h after [F-18]FLT administration with a 10% post-voiding residual; urine reaccumulation between 2 and 6 h at a rate determined by the bladder curve fit; second bladder voiding at 6 h with a 10% post-voiding residual decayed to infinity. This scenario assumed no urine reaccumulation after 6 h. The first scenario is conservative, whereas the second has a more realistic voiding scheme.

VII. [F-18]FLT PREVIOUS HUMAN EXPERIENCE

Preliminary studies using [F-18]FLT for imaging human subjects have been published (Table 13). [F-18]FLT has been studied for imaging in Germany and in the United States (UCLA, University of Washington in Seattle, Wayne State University). Imaging protocols used in Germany and the US were pre-approved by their respective regulating committees and done under the RDRC process. Patients received from 1.4-11 mCi of [F-18]FLT. Some imaging results have been published (Table 13). The most experience in the United States with the imaging agent is from the group in Seattle where numerous patient studies have been performed in patients with lung cancer and in a few with primary brain tumors. The images demonstrate the feasibility and merit of tumor imaging with [F-18]FLT. [F-18]FLT PET showed increased uptake in tumor lesions outside the liver or bone marrow (standardized uptake value (SUV) 4-7), which were delineated from surrounding tissue (SUV 0.5-2).

These and other studies are tabulated in Table 13 below.

Table 13. A Summary of published manuscripts reporting [F-18]FLT human imaging studies.

	Organ system	N	mCi injected	MBq Injected (mean)	Specific Activity	Reference
2009	GI	21	0.18	3.5 MBq/Kg	Not Reported	Kameyama (2009)
2009	Brain	14	5.4	200	Not Reported	Price (2009)
2008	Lung	9	7.9-10.5	292-389(373)	210 GBq/umol	Shields (2008)
2008	Lung	28	15	555	3,225-7,672 Ci/umol	Sohn (2008)
2008	Lung/HN	9/6	10	370	Not Reported	De Langen (2008)
2008	Blood	10	7.1-10	265-370 (334)	Not Reported	Buck (2008)
2008	Pancreas	31	7.3-9.2	270-340	Not Reported	Herrmann (2008)
2008	Lung	54	2.7-6.4	101-238 (158)	Not Reported	Yamamoto (2008)
2008	GI	5	8.7-12.7	328-470	Not Reported	Roels (2008)
2008	Lung	34	8.1-10.8	300-400	Not reported	Yamamoto (2008)
2008	Bone & soft tissue	22	9.5-11.5	350-425	120GBq/mmol	Buck (2008)
2008	Pancreas	5	5.2-7	192-259	Not reported	Quon (2008)
2008	Brain	13	8.7	322±85	Not reported	Ullrich (2008)
2007	Brain	21	0.05 mCi/kg	2.0 MBq/kg	Not reported	Chen (2007)
2007	Gastric	45	7.3-9.2	270-340	Not reported	Herrmann (2007)
2007	Breast	15	4.1-10.3	153-381	15-227 GBq/mmol	Kenny (2007)
2007	Brain	9	0.04 mCi/kg	1.5 MBq/kg	Not reported	Schiepers (2007)
2007	Lung	55	8.1-10.8	300-400	Not reported	Tian (2007)
2007	Lung	20	0.07 mCi/kg	2.6 MBq/kg	Not reported	Turcotte (2007)
2008	Brain	41	Mean 4.35 3.49-6.38	Mean 161 129-236	Not reported	Hatakeyama (2008)
2008	Brain	12	Mean 4.74 4.16-5.19	Mean 175 154-192	Mean 3594 mCi/mmol 1250-10,000	Spence (2008
2008	Lung	54	Mean 3.51 2.73-6.43	101-238	Not reported	Yamamoto (2008)

2007	Lung	18	3.92	145±26	Not reported	Yamamoto (2007)
2007	Sarcoma	10	Mean 9.81 3.24-11.62	Mean 363 120-430	Not reported	Been (2007)
2007	Lymphoma	21	Mean 8.11 7.20-9.19	Mean 300 270-340	Not reported	Herrmann (2007)
2007	Head/Neck	10	6.76	250	10TBq/mmol	Troost (2007)
2007	Lymphoma	48	3.9	148.6	Not reported	Kasper (2007)
2007	Rectal	10	8.1	300	Not reported	Wieder (2007)
2006	Bone marrow	18	10.8	400	10TBq/mmol	Agool (2006)
2006	Brain	12	5	185	7.4GBq/µmol	Muzi (2006)
2006	Brain	10	Mean 4.0 2.8-5.4	Mean 150 104-202	37GBq/µmol	Yamamoto (2006)
2006	Brain	25	10	370	Not reported	Saga (2006)
2006	Lymphoma	34	Mean 9.3 7.1-10	Mean 345 265-370	Not reported	Buck (2006)
2006	Breast	10	4.3-11.3	160-420	>10TBq/mmol	Been (2006)
2006	Lung	11	5.0	185	Not reported	Yap (2006)
2005	Lung	47	7.2-10.0	265-370	Not reported	Buck (2005)
2005	Brain	25	Mean: 4.7 3.8-5.9	Mean 174 141-218	74TBq/mmol	Chen (2005)
2005	Brain	26	10	370	3.2-7.7 Ci/µmol	Choi (2005)
2005	Brain	25	Mean 8.7 3.0-10.0	Mean 322 111-370	Not reported	Jacobs (2005)
2005	Breast	15	4.1-10.5	153-389	25-465 GBq/µmol	Kenny (2005)
2005	Lung	17	Max 5 0.07/kg	Max 185 2.6 /kg	>37 GBq/mmol	Muzi (2005)
2005	Breast	14	3.5	130	74 TBq/mmol	Pio (2005)
2005	All	33	Mean 9.5 8.4-9.7	Mean 350 310-360	>220 GBq/mmol	Shields (2005)
2005	Esophagus	10	Mean 11.0 9.2-12-2	Mean 410 340-450	>10 TBq/mmol	Van Westreenen (2005)

2004	Lymphoma	7	4.3 -13.2	Mean = 324 159 - 489	Not reported	Buchmann 2004
2004	Lung	17	5.7	Mean=210 130-420	>10TBq/mmol =10GBq/umol	Cobben 2004
2004	Lung	28 (a)	9	Mean=334 265-370	Not reported	Halter 2004
2004	Breast	12	8.1-12.1	300-450	Not reported	Smyczek-Gargya 2004
2004	Colorectal	18	9.7	360 ± 25	Not reported	Visvikis 2004
2004	Heent	21	9.2	Mean=340 165-650	>10TBq/mmol =10GBq/umol	Cobben 2004
2004	Soft tissue	19	10.8	Mean=400 115 -430	>10TBq/mmol =10GBq/umol	Cobben 2004
2003	Lymphoma	11	7.5	280	Not reported	Wagner 2003
2003	Colorectal	10 (b)	9.5	351 ± 52	Not reported	Francis 2003)
2003	Colorectal	17 (b)		Mean=360 312-412	Not reported	Francis 2003
2003	Dosimetry	18	5.0	185 MBq max	> 37 GBq/umol	Vesselle 2003
2003	Lung	16	5.4 -10.8	200 - 400	Not reported	Dittman 2003
2003	Melanoma	10	10.8	Med= 400 185-430	>10TBq/mmol =10GBq/umol	Cobben 2003
2003	Lung	26 (c)	9.0	Mean=334 265-370	Not reported	Buck 2003
2002	Lung	30 (c)	9.0	Mean=334 265-370	Not reported	Buck 2002
2002	Lung	10	5.0	185 max	> 1Ci/umol = 37GBq/umol	Vesselle 2002
	Total no. Subjects:	1054*				

(a) There appear to be 10 additional unique patients that were not described in the Buck 2002 and 2003 manuscripts.
(b) It is unclear if the same patients are being described for both of the Francis manuscripts.

(c) It is unclear if the same patients are being described for both of the Buck, 2002 and 2003, manuscripts.
* Due to the possibility that the same patients are being described in some reports the total # of unique patients studied in these published studies appears to be 670.

As one can see from the information in Table 13 many of the published studies did not specifically mention the specific activity of the [F-18]FLT so it is not possible to actually assess the amount of FLT that was actually administered to the patient. Furthermore only the Turcotte and Spence papers have specifically addressed safety issues by describing laboratory results post injection or assess for neurological sequelae such as mild peripheral neuropathy. This is addressed in section 6 where 2 studies with safety monitoring are detailed.

VIII. REFERENCES

Agool A, Schot BW, Jager PL, Vellenga E. 18F-FLT PET in Hematologic Disorders. J Nucl Med 2006; 47(10):1592-98.

Ammonul, NDA # 020645, approved product labeling, 2005

Anonomous. Final report on the safety assessment of Benzyl alcohol, benzoic acid, and sodium benzoate. Int J Toxicol; 2001 20(3 suppl):23-50.

Bading J, Shields A. Imaging of Cell Proliferation: Status and Prospects. The J. Nucl. Med 2008; 49, No. 6 suppl.

Been LB, Elsinga P H. "Positron emission tomography in patients with breast cancer using (18)F-3'-deoxy-3'-fluoro-l-thymidine ((18)F-FLT)-a pilot study." Eur J Surg Oncol 2006 32(1):39-43.

BeenLB, Suurmeijer AJH, Elsinga PH, Jager PL, Ginkel RJV, Hoekstra HJ. ^{18}F-Fluorodeoxythymidine PET for Evaluation the Response to Hyperthermic Isolated Limb Perfusion for Locally Advanced Soft-Tissue Sarcomas. J Nucl Med 2007; 48:367-372.

Buchmann I, Neumaier Bernd, Schreckenberger M, Reske S. [^{18}F]3'-Deoxy-3'-Fluorothymidine-PET in NHL Patients. Cancer Biotherapy and Radiopharmaceuticals 2004; 19:436-442.

Buck AK, Bommer M, Stilgenbauer S, Juweid M, Glatting G, Schirrmeister H, Mattfeldt T, Tepsic D, Bunjes D, Mottaghy FM, Krause BJ, Neumaier B, Dohner H, Moller P, Reske SN. Molecular Imaging of Proliferation in Malignant Lymphoma. Cancer Res 2006; 66:(22)11055-61.

Buck AK, Schirrmeister H, Hetzel M, Heide MV, Halter Gisela, Glatting G, Mattfeldt T, Liewald F, Reske SN, Neumaier B. 3-Deox-3-[^{18}F] Fluorothymidine-Positron Emission Tomography for noninvasive Assessment of Proliferation in Pulmonary Nodules. Cancer Research 2002; 62:3331-3334.

Buck AK, Halter G, Schirrmeister H, Kotzerke J, Wurziger I, Glatting G, Mattfeldt T, Neumaier B, Reske SN, Hetzel M. Imaging Proliferation in Lung Tumors with PET: 18F-FLT Versus 18F-FDG. J Nucl Med 2003; 44:1426-1431.

Buck AK and Hetzel M. Clinical relevance of imaging proliferative activity in lung nodules. Eur J Nucl Med Mol Imaging 2005; 32(5):525-33.

Buck AK, Hermann K, Buschenfelde CMZ, Juweid ME, Bischoff M, Glatting G, Weirch G, Moller P, Wester HJ, Scheidhauer K, Dechow T, Peschel Ch, Schwaiger M, Reske SN. Imaging Bone and Soft Tissue Tumors with the Proiferation Marker [18F] Fluorodeoxythymidine. Clin Cancer Res 2008; 14(10).

Andreas K. Buck, Martin Bommer, Malik E. Juweid, Gerhard Glatting, Stephan Stilgenbauer, Felix M. Mottaghy, Melanie Schulz, Thomas Kull, Donald Bunjes, Peter Moller, Hartmut Dohner, and Sven N. Reske. First Demonstration of Leukemia Imaging with the Proliferation. J Nucl Med 2008; 49(11).

Channing MA, Huang BX, Eckelman WC. Analysis of residual solvents in 2-[18F]FDG by GC. Nuclear Medicine and Biology 2001; 28:469-471.

Chen W, Cloughesy T. Imaging proliferation in brain tumors with 18F-FLT PET: comparison with 18F-FDG. J Nucl Med 2005 46(6):945-52.

Chen W, Delaloye S, Silverman DHS, Geist Ch, Czernin J, Sayre J, Satyamurthy N, Pope W, Lai A, Phelps ME, Cloughesy T. Predicting Treatment Response of Malignant Gliomas to Bevacizumab and Irinotecan by Imaging Proliferation with [18F] Fluorothymidine. J of Clin Onc 2007; Vol 25.

Choi SJ, Kim JS. [18F]3'-deoxy-3'-fluorothymidine PET for the diagnosis and grading of brain tumors. Eur J Nucl Med Mol Imaging 2005 32(6):653-9.

Cobben DCP, Elsinga PH, Suurmeijer AJH, Vaalburg W, Maas B, Jager PL, Hoekstra HJ. Detection and Grading of Soft Tissue Sarcomas of the Extremities with 18F-3'-Fluoro-3'-Deoxy-L-Thymidine. Clinical Cancer Research 2004; 10:1685-1690.

Cobben DCP, Jager PL, Elsinga PH, Maas B, Suurmeijer AJH, Hoekstra HJ. 3'-18F-Fluoro-3'-Deoxy-L-Thymidine. A New Tracer for Staging Metastatic Melanoma? J Nucl Med 2003; 44:1927-1932.

Cobben DCP, van der Laan BFAM, Maas B, Vaalburg W, Suurmeijer AJH, Hoekstra HJ, Jager PL, Elsinga PH. 18F-FLT PET for Visualization of Laryngeal Cancer: Comparison with 18F-FDG PET. J Nucl Med 2004; 45:226-231.

Adrianus J. de Langen, Bianca Klabbers, Mark Lubberink, Ronald Boellaard, Marieke D. Spreeuwenberg, Ben J. Slotman, Remco de Bree, Egbert F. Smit, Otto S. Hoekstra, Adriaan A. Lammertsma. Reproducibility of Quantitative ^{18}F-3'-deoxy-3'-Fluorothymidine. Eur J Nucl Med Mol Imaging, 2008.

Dittmann H, Dohmen BM, Kehlbach R, Bartusek G, Pritzkow M, Sarbia M, Bares R. Early changes in [(18)F]FLT uptake after chemotherapy: an experimental study. European Journal of Nuclear Medicine Molecular Imaging 2002; 29(11):1462-9.

Dittmann H, Dohmen BM, Paulsen F, Eichhorn K, Eschmann SM, Horger M, Wehrmann M, Machulla HJ, Bares R. [18F]FLT PET for diagnosis and staging of thoracic tumours. European Journal of Nuclear Medicine Molecular Imaging 2003; 30:1407-1412.

Dreisbach RH and Robertson WO. Handbook of poisoning: prevention, diagnosis and treatment; 12th ed. p 171-4, Appleton and Lange Publ., Los Altos (CA), 1987.

Faraj A, Fowler DA, Bridges EG, Sommadossi JP. Effects of 2',3'-dideoxynucleosides on proliferation and differentation of human pluripotent progenitors in liquid culture and their effects on mitochondrial DNA synthesis. Antimitcrobial Agent Chemother 1994; 38(5):924-930.

FDA Guidance for Industry ICH Q3C—Tables and List (November 2003 Revision 1

Flexner C, van der Horst C, Jacobson MA. Relationship between plasma concentrations of 3'-deoxy-3'-fluorothymidine (Alovudine) and antiretroviral activity in two concentration-controlled trails. J Infec Dis 1994; 170:1394-1403.

Francis DL, Freeman A, Visvikis D, Costa C, Luthra SK, Novelli M, Taylor I, Ell PJ. In vivo imaging of cellular proliferation in colorectal cancer using positron emission tomography. Gut 2003; 52: 1602-1606.

Francis DL, Visvikis D, Costa DC, Arulampalam THA, Townsend C, Luthra SK, Taylor I, Ell PJ. Potential impact of [18F]3′-deoxy-3′-fluorothymidine versus [18F]fluoro-2-deoxy-D-glucose in positron emission tomography for colorectal cancer. European Journal of Nuclear Medicine Molecular Imaging 2003; 30:988-994.

Grierson JR and Shields AF. Radiosynthesis of 3'-deoxy-3'-[(18)F]fluorothymidine: [(18)F]FLT for imaging of cellular proliferation in vivo. Nucl Med Biol 2000; 27(2):143-56.

Halter G, Buck AK, Schirrmeister H, Wurziger I, Liewald F, Glatting G, Neumaier B, Sunder-Plassmann L, Reske SN, Hetzel M. [18F] 3-deoxy-3′-fluorothymidine positron emission tomography: alternative or diagnostic adjunct to 2-[18f]-fluoro-2-deoxy-D-glucose positron emission tomography in the workup of suspicious central focal lesions? Journal of Thoracic and Cardiovascular Surgery; 127 (4):1093-1099, 2004.

Hatakeyama T, Kawai N, Nishiyama Y, Yamamoto Y, Sasakawa Y, Ichikawa T, Tamiya T. ^{11}C-methionine (MET) and ^{18}F-Fluorothymidine (FLT) PET in Patients with newly diagnosed glioma. Eur J Nucl Med Mol Imaging 2008.

Hermann K, Ott K, Buck AK, Lordick F, Wilhelm D, Souvatzoglou M, Becker K, Schuster T, Wester HJ, Siewert JR, Schwaiger M, Krause BJ. Imaging Gastric Cancer with PET and Radiotracers [18F]-FLT and [18F]-FDG. J Nucl Med 2007; 48:1945-1950.

Herrmann K, Wieder HA, Buck AK, Schoffel M, Krause BJ, Fend F, Schuster T, Buschenfelde CMZ, Wester HJ, Duyster J, Peschel C, Schwaiger M, Dechow T. Early Response Assessment using 3'-Deoxy-3'-[^{18}F] Fluorothymidine Positron Emission Tomography in High-Grade Non-Hodgkin's Lymphoma. Clin Cancer Res 2007; 13(12).

Ken Herrmann, Florian Eckel, Stefan Schmidt, Klemens Scheildhauer, Bernd Joachim Krause, Joerg Kleeff, Tibor Schuster, Hans-Juergen Wester, Helmut Friess, Roland M. Schmid, Markus
Schwaiger, and Andreas K. Buck. In Vivo Characterization of Proliferation. J Nucl Med 2008; 49:1437-1444.

Jacobs AH and Thomas A. 18F-fluoro-L-thymidine and 11C-methylmethionine as markers of increased transport and proliferation in brain tumors. J Nucl Med 2005; 46(12):1948-58.

Jung AL, Roan Y, Temple AR. Neonatal death associated with acute transplacental ethanol intoxication, Am J Dis Child 1980; 134:419-20.

Kameyama R, Yamamoto Y, Izuishi K, Takebayashi R, Masanobu H, Makiko M, Masato K, Haba R, Nishiyama Y. Detection of gastric cancer using ^{18}F-FLT PET: comparison with ^{18}F-FDG PET. Eur J Nucl Med Mol Imaging 2009, 36:382-388.

Katlama Ch, Ghosn J, Tubiana R, Wirden M, Valantin MA, Harmenberg J, Mardh G, Oberg B, Calvez V. MIV-310 reduces HIV viral load in patients failing multiple antiretroviral therapy: results from a 4-week phase II study. AIDS 2004; 18:1299-1304.

Kasper B, Egerer G, Gronkowski M, Haufe S, Lehnert T, Eisenhut M, Mechtersheimer G, Ho AD, Haberkorn U. Functional diagnosis of residual lymphomas after radiochemotherapy with positron emission tomography comparing FDG- and FLT PET. Leukemia & Lymphoma, 2007:48(4):746-753.

Kenny LM and Vigushin DM. Quantification of cellular proliferation in tumor and normal tissues of patients with breast cancer by [18F]fluorothymidine-positron emission tomography imaging: evaluation of analytical methods. Cancer Res 2005 65(21):10104-12.

Kenny L, Coombes Ch, Vigushin DM, Sami Shousha AA, Aboagye EO. Imaging early changes in proliferation at 1 week post chemotherapy: a pilot study in breast cancer patients with 3'-deoxy-3'-[18F]Fluorothymidine positron emission tomography. Eur J Nucl Med Mol Imaging 2007; 34:1339-1347.

Kong XB, Zhu QY, Vidal PM. Comparisons of anti-human immunodeficiency virus activities, cellular transport, and plasma intracellular pharmacokinetics of 3'-fluoro-3'-deoxythymidine and 3'-azido-3'-deoxythymidine. Antimicrob Agents Chemo 1992; 36(4):808-18.

Kupiecki FP and Coon MJ, Biochem. Prep 1960; 7:69-71.

Langen P and Graetz H. Cell death resulting from inhibition by 3'-deoxy-3'-fluorothymidine, cytosine-arabinoside, 5-fluoro-2'-deoxyuridine, and hydroxyurea of DNA synthesis in cultured Ehrich ascites carcinoma cells. Studia Biophys 1972; 31/32:359-366.

Langen P, Etzold G, Hintsche R, Kowollik G: 3'-Deoxy-3'-fluorothymidine, a new selective inhibitor of DNA synthesis. Acta Biol Med Germ 1969; 23:759-766.

Langen P, Kowollok G, Etzold G, Venner H, Reinhert H. The phosphorylation of 3'-deoxy-3'-fluorothymidine and its incorporation into DNA in a cell free system from tumor cells. Acta Biol Med Germ 1972; 29:483-494.

Lu L, Samuelsson L, Bergstrom M, Sato K, Fasth KJ, Langstrom B. Rat studies comparing 11C-FMAU, 18F-FLT, and 76Br-BFU as proliferation markers. J Nucl Med 2002; 43(12):1688-98.

Lundgren B, Bottiger D, Ljungdahl-Stahle. Antiviral effects of 3'-fluorothymidine and 3'-azidothymidine in Cynomolgus monkeys infected with simian immunodeficiency virus. J Acq Immunodef Synd 1991; 4(5):489-498.

Machulla H.J. Procedure for Routine Synthesis of [18F]FLT in High Activities. J. Nucl. Med 2001; 42 (5), 257P.

Matthes E, Lehmann Ch, Scholz D, Rosenthal HA and Langen P. Phosphorylation, anti-HIV activity and cytotoxicity of 3'-fluorothymidine. Biochem Biophys Res Comm 1998; 153(2):825-831.

Matthes E, Lehmann Ch, Scholz D, von Janta-Lipinski M, Gaertner K, Rosenthal HA, Langen P. Inhibition of HIV-associated reverse transcriptase by sugar modified derivatives of thymidine 5'-triphosphate in comparison to cellular DNA polymerases. Biochem Biophys Res Comm 1987; 148(1):78-85.

Mock BH, Winkle W, Vavrek MT. Technical Note: A Color Spot Test for the Detection of Kryptofix® [2.2.2] in [18F]FDG Preparations. Nuclear Medicine & Biology 1997; 24:193-195.

Muzi M, Vesselle H. Kinetic analysis of 3'-deoxy-3'-fluorothymidine PET studies: validation studies in patients with lung cancer. J Nucl Med 2005 46(2):274-82.

Muzi M, Spence AM, O'Sullivan F, Mankoff DA, Wells MW, Grierson JR, Link JM, Krohn KA. Kinetic Analysis of 3' – Deoxy-3' – 18F- Flourothymidine in Patients with Gliomas. J Nucl Med 2006; 47(10) 1612-21.

Pio BS, Park CK. Usefulness of 3'-[F-18]Fluoro-3'-deoxythymidine with Positron Emission Tomography in Predicting Breast Cancer Response to Therapy. Mol Imaging Biol 2005; 1-7.

S.J. Price, T.D. Fryer, M.C. Cleij, A.F. Dean, J. Joseph, R. Salvador, D.D. Wang, P.J. Hutchinson, J.C. Clark, N.G. Burnet, J.D. Pickard, F.I. Aigbirhio, J.H. Gillard, Imaging regional variation of cellular proliferation in gliomas using 30-deoxy-30-[18F]fluorothymidine positron-emission tomography: an image-guided biopsy study. Clinical Radiology (2009); 64:52-63.

Quon A, Chang ST, Chin F, Kamaya A, Dick DW, Loo Jr BW, Gambhir SS, Koong AC. Initial Evaluation of [18F]-Fluorothymidine (FLT) PET/CT scanning for primary pancreatic cancer. Eur J Nucl Med Mol Imaging 2008; 35:527-531.

Rasey JS, Grierson JR, Wiens LW, Kolb PD, Schwartz JL. Related Articles, Validation of FLT uptake as a measure of thymidine kinase-1 activity in A549 carcinoma cells. J Nucl Med.Sep 2002; 43(9):1210-7.

Sarah Roels, Pieter Slagmolen, Johan Nuyts, John A. Lee, Dirk Loeckx, Frederik Maes, Sigrid Stroobants, Freddy Penninckx, and Karin Haustermans. Biological Image-guided dradiotherapy in rectal cancer. Acta Oncologica, 2008; 47: 1237-1248.

Shaw G and Warrener RN, J. Chem. Soc; 153-156, 1958

Schiepers Ch, Chen W, Dahlbom M, Cloughesy T, Hoh CK, Huang S-Ch. [18F]-Fluorothymidine Kinetics of Malignant Brain Tumors. Eur J Nucl Med Mol Imaging 2007; 34: 1003-1011.

Shields AF, Grierson JR, Dohmen BM, Machulla HJ, Stayanoff JC, Lawhorn-Crews JM, Obradovich JE, Muzik O, Mangner TJ. Imaging proliferation in vivo with [F-18]FLT and positron emission tomography. Nat Med 1998; 4(11):1334-6.

Shields AF and Briston DA. A simplified analysis of [18F]3'-deoxy-3'-fluorothymidine metabolism and retention. Eur J Nucl Med Mol Imaging 2005; 32(11):1269-75.

Anthony F. Shields, Jawana M. Lawhorn-Crews, David A. Briston, Sajad Zalzala, Shirish Gadgeel, Kirk A. Douglas, Thomas J. Mangner, Lance K. Heilbrun, and Otto Muzik. Analysis and Reproducibility of 3'-Deoxy-3' –[^{18}F] Fluorothymidine. Clin Cancer Res 2008; 14(14).

Smyczek-Gargya B, Fersis N, Dittmann H, Vogel U, Reischl G, Machulla HJ, Wallwiener D, Bares R, Dohmen BM. PET with [18F]fluorothymidine for imaging of primary breast cancer: a pilot study. European Journal of Nuclear Medicine Molecular Imaging 2004; 31:720–724.

Saga Tsuneo, Kawashima H, Araki N, Takahashi JA, Nakashima Y, Higashi T, Oya N, Mukai T, Hojo M, Hashimoto N, Manabe T, Hiraoka M, Togashi K. Evaluation of Primary Brain Tumors with FLT-PET Usefulnes and Limitation. Clinical Nucl Med 31 2006; 774-80.

Hee-Jung Sohn, You-Jung Yang, Jin-Sook Ryu, Seung Jun Oh, Ki Chun Im, Dae Hyuk Moon, Dae Ho Lee, Cheolwon Suh, Jung-Shin Lee, and Sang-We Kim. [^{18}F] Fluorothymidine Positron Emission Tomography before and 7 days after Gefitinib Treatment. Clin Cancer Res 2008; 14(22).

Spence A, Muzi M, Link J, Hoffman J, Eary J, Krohn K. NCI-Sponsored Trial for the Evaluation of Safety and Preliminary Efficacy of FLT as a Marker of Proliferation in Patients with Recurrent Gliomas. Safety Studies. Mol Imaging Biol:2008.

Sundseth R, Joyner SS, Moore JT, Dornsife RE, Dev IK. The anti-human immunodeficiency virus agent 3'-fluorothymidine induces DNA damage and apoptosis in human lymphoblastiod cells. Antimicrob Agents Chemother 1996; 40(2):331-335.

Tian J, Yang X, Yu L, Chen P, Xin J, Ma L, Feng H, Tan Y, Zhao Z, Wu W. A multicenter Clinical Trial on Diagnostic Value of Dual-Tracer PET/CT in Pulmonary Lesions Using 3'-Deoxy-3'-[18F]-Fluorothymidine and [18F]-FDG. J Nucl Med 2008; Vol. 49 No. 2.

Troost Esther GC, Vogel WV, Merkx MAW, Slootweg PJ, Marres HAM, Peeters WJM, Bussink J, Kogel AV, Oyen WJG, Kaanders JHAM. 18F-FLT PET does not discriminate between reactive and metastic lymph nodes in primary head and neck cancer patients. J Nucl Med 2007; 48(5):726-35.

Turcotte E, Linda Wiens L, Grierson J, Peterson L, Wener MH, Vesselle H. Toxicology Evaluation of Radiotracer Doses of 18F-FLT (3'-deoxy-3' fluorothymidine) for Human PET Imaging (In press).

Van Westreenen HL, Cobben DC. Comparison of 18F-FLT PET and 18F-FDG PET in esophageal cancer. J Nucl Med 2005 46(3):400-4.

Turcotte E, Wiens LW, Grierson JR, Peterson LM, Wener MH, Vesselle H. Toxicology evaluation of radiotracer doses of 3'-deoxy-3'-[18F]Fluorothymidine (18F-FLT) for human PET Imaging. BMC Nucl Med; 2007; 7:3.

Ullrich R, Backes H, Li H, Kracht L, Miletic H, Kesper K, Neumaier B, Heiss WD, Wienhard K, Jacobs AH. Glioma Proliferation as Assessed by 3'-Fluoro-3'-Deoxy-L-Thymidine Positron Emission Tomography in patients with newly diagnosed high-grade glioma. Clin Cancer Res 2008; 14(7).

Vesselle H, Grierson J, Muzi M, Pugsley JM, Schmidt RA, Rabinowitz P, Peterson LM, Vallieres E, Wood DE. In Vivo Validation of 3'deoxy-3'-[(18)F]fluorothymidine ([(18)F]FLT) as a Proliferation Imaging Tracer in Humans: Correlation of [(18)F]FLT Uptake by Positron Emission Tomography with Ki-67 Immunohistochemistry and Flow Cytometry in Human Lung Tumors. Clin Cancer Res 2002; 11:3315-23.

Vesselle H, Grierson J, Peterson LM, Mark Muzi M, Mankoff DA, and Krohn KA. 18F-Fluorothymidine Radiation Dosimetry in Human PET Imaging Studies. J Nucl Med 2003; 44:1482–1488.

Visvikis D, Francis D, Mulligan R, Costa DC, Croasdale I, Luthra SK, Taylor I, Ell PJ. Comparison of methodologies for the in vivo assessment of 18FLT utilisation in colorectal cancer. European Journal of Nuclear Medicine Molecular Imaging 2004; 31:169-178.

Wagner M, Seitz U, Buck A, Neumaier B, Schultheiß S, Bangerter M, Bommer M, Leithäuser F, Wawra E, Munzert G, Reske SN. 3'-[18F]Fluoro-3'-Deoxythymidine ([18F]-FLT) as Positron Emission Tomography Tracer for Imaging Proliferation in a Murine B-Cell Lymphoma Model and in the Human Disease. Cancer Research 2003; 63: 2681-2687.

Wieder Hinrich A, Geinitz H, Rosenberg R, Lordic F, Becker K, Stahl A, Rummeny E, Siewert JR, Schwaiger M, Stollfuss J. PET imaging with [18F]3'-deoxy-3'-fluorothymidine for predication of response to neoadjuvant treatment in patients with rectal cancer. Eur J Nucl Med Mol Imaging 2007; 34:878-883.

Wobus AM. Clastogenic activity of cytosine arabinoside and 3'-deoxy-3'-fluorothymidine in Ehrlich acites tumor cells in vitro. Mutation Res 1976; 40:101-106.

Yap, CS and Czernin J. Evaluation of Thoracic Tumors With 18F-Fluorothymidine and 18F- Fluorodeoxyglucose-Positron Emission Tomography. Chest 2006; 129(2): 393-401.

Yamamoto Y, Wong TZ, Turkington TG, Hawk TC, Reardon DA, Coleman RE. 3'-Deoxy-3'-[F-18]Fluorothymidine positron emission tomography in patients with recurrent glioblastoma multiforme: comparison with GD-DTPA enhanced magnetic resonance imaging. Mol Imaging Biol 2006; 8:340-47.

Yamamoto Y, Nishiyama Y, Ishikawa S, Nakano J, Chang SS, Bandoh S, Kanaji N, Haba R, Kushida Y, Ohkawa Motoomi. Correlation of ^{18}F-FLT and ^{18}F-FDG uptake on PET with Ki-67 immunohistochemistry in non-small cell lung cancer. Eur J Nucl Med Mol Imaging 2007; 34:1610-1616.

Yamamoto Y, Nishiyama Y, Kimura N, Ishikawa S, Okuda M, Bandoh S, Kanaji N, Asakura M, Ohkawa M. Comparison of ^{18}F-FLT PET and ^{18}F-FDG PET for preoperative staging in non-small cell lung cancer. Eur J Nuc Med Mol Imaging 2008; 35:236-245.

Yamamoto Y, Nishiyama Y, Kimura N, Ishikawa Sh, Okuda M, Bandoh Sh, Kanaji N, Asakura M, Ohkawa M. Comparison of [18F]-FLT PET and [18F]-FDG PET for preoperative staging in non-small cell lung cancer. Eur J Nucl Med Mol Imaging 2008; 35: 236-245.

Yuka Yamamoto, Yoshihiro Nishiyama, Shinya Ishikawa, Masashi Gotoh, Shuji Bandoh, Nobuhiro Kanaji, Masato Asakura, and Motoomi Ohkawa. 3'-Deoxy-3'-^{18}F-Fluorothymidine as a Proliferation Imaging Tracer for Diagnosis of Lung Tumors. Comput Assist Tomogr 2008 32(3).

Yun M, Oh SJ, Ha HJ, Ryu JS, Moon DH. High radiochemical yield synthesis of 3'-deoxy-3'-[18F]fluorothymidine using (5'-O-dimethoxytrityl-2'-deoxy-3'-O-nosyl-beta-D-threo pentofuranosyl)thymine and its 3-N-BOC-protected analogue as a labeling precursor. Nucl Med Biol 2003; 30(2):151-7.